

Dissymmetric On-Surface Dehalogenation Reaction Steered by Preformed Self-Assembled Structure

Hui Lu,¹ Wenlong E,¹ Liangliang Cai, Zhibo Ma,^{*} Wei Xu,^{*} and Xueming Yang^{*}

Cite This: *J. Phys. Chem. Lett.* 2020, 11, 1867–1872

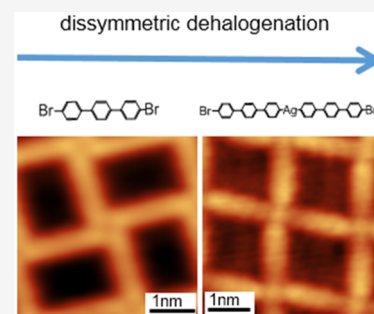
Read Online

ACCESS |

Metrics & More

Article Recommendations

ABSTRACT: Ullmann coupling of 4,4''-dibromo-*p*-terphenyl (DBTP) thermally catalyzed on a Ag(111) surface was studied by scanning tunneling microscopy. Detailed experimental measurement shows that the Ullmann coupling reaction pathways of DBTP molecules can be controlled by pre-self-assembly, and the dissymmetric dehalogenation reaction is realized. Moreover, self-assembly of the reactants in a rectangular network undergoes a dissymmetric debromination transfer to a newly observed rhombic network formed by organometallic dimers prior to the formation of longer symmetric organometallic intermediates on a Ag(111) surface, while the ladder assembled phase is more likely to induce the symmetric debromination reaction and converts into the symmetric organometallic intermediate. These findings help us to understand the essentials of the dissymmetric dehalogenation reaction that originated from a symmetric compound and pave new avenues for advancing the emerging field of on-surface synthesis.



The recently developed on-surface synthesis strategy, by which well-defined robust molecular structures can be prepared on surfaces via covalent coupling, has spurred much interest in recent years. In comparison with the traditional solution chemistry, the on-surface synthesis strategy is particularly attractive owing to its following characteristics. (i) It is relatively easy to control the reaction results from properly designed precursor molecules on surfaces. (ii) Due to the steric confinement and the catalytic ability of surfaces, some unexpected reactions that are inhibited in wet chemistry can occur.^{1–3} Thus, this strategy has opened up a new avenue for the fabrication of numerous novel nanostructures. To improve our understanding of atomic-scale structural assignments and detailed electronic properties, products of on-surface synthesis can be investigated by scanning tunneling microscopy and spectroscopy (STM and STS),^{4,5} noncontact atomic force microscopy (nc-AFM),^{6,7} and X-ray photoelectron spectroscopy (XPS).⁸ So far, various chemical reactions have been successfully performed on metal surfaces under ultra-high-vacuum (UHV) conditions, such as homo-coupling of terminal alkynes,^{9–11} cyclodehydrogenation,^{12,13} and C–H activation.^{14–16} Nevertheless, due to its relative reliability and controllability, the Ullmann-type reaction of halogenated aromatic molecules has attracted a great deal of attention and is currently considered as one of the most appropriate approaches to build up complicated as well as robust molecular structures on surfaces.^{17–20} Some STM studies have revealed that an organometallic compound with carbon–metal–carbon bonds can be the intermediate product of Ullmann coupling,^{21–23} and bright circular protrusions amidst molecular units in the STM topography are clearly

discernible and readily identified as inserted metal atoms.²⁴ As extensively reported in prior work, this kind of organometallic intermediate plays an important role in the Ullmann reaction and can provide details of the reaction mechanism.^{25,26} In addition, as has been demonstrated, the Ullmann reaction can be seriously influenced by some key factors like substrate surfaces,²⁰ surface reconstruction,²⁷ and step edges.²⁸ Typically, several studies have reported that the self-assembly of reactants can also efficiently steer Ullmann reactions.²⁹ Symmetric halogenated precursors, which contain multiple halogen atoms of the same chemical environment, are widely used in the on-surface Ullmann synthesis of hydrocarbon polymers such as graphene nanoribbons³⁰ and nanoporous graphene.²⁰ However, most works reported only the formation of full debromination products of those symmetric precursors, and there might be evidence of the dissymmetric debromination reaction hiding in the stepwise process of dehalogenation. The study of dissymmetric chemical reaction of multiple equivalent reacting sites within one molecule is very important for synthetic chemistry and material science. Most recently, the on-surface dissymmetric reaction of 1,4-dibromo-2,5-diethynylbenzene on Ag(111) through a stepwise activation strategy has been reported, which leads to dissymmetric reactions of two equivalent Br-substituted sites in the molecule.³¹ In addition to the dissymmetric reaction caused by a stepwise

Received: December 12, 2019

Accepted: February 19, 2020

Published: February 19, 2020

Scheme 1. Two Reaction Pathways of the DBTP Molecule on a Ag(111) Surface

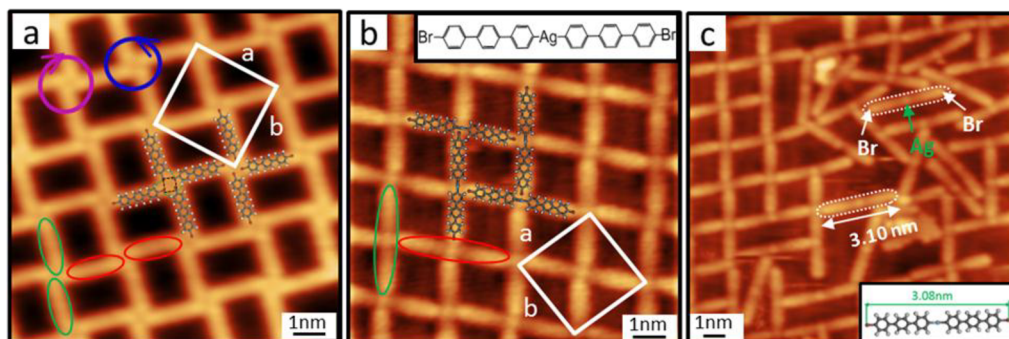
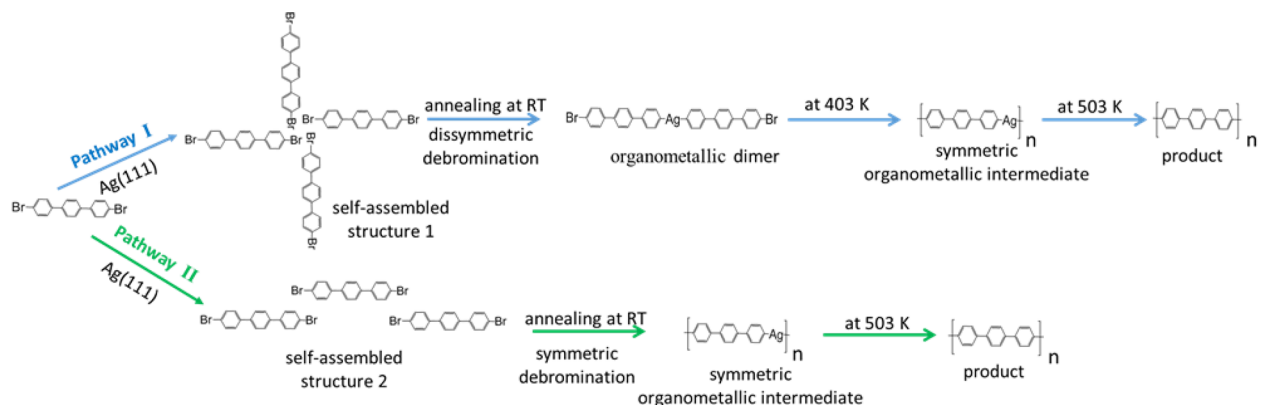


Figure 1. (a) Typical STM image of a rectangular network after DBTP molecules have been deposited on a cold Ag(111) surface for 5 min. (b) STM image of the ordered rhombic network after thermal annealing at RT for 2 h. The unit cell is indicated by the white rhombus. The corresponding structural models are overlaid on the corresponding STM topography. (c) STM image of two coexisting structures: ordered rhombic network and ambient dispersed dimers. Dimer products are highlighted by white contours. White for H, gray for C, and red for Br. (a) $U = -1.10$ V, and $I = 17.0$ pA. (b) $U = -1.03$ V, and $I = 32.7$ pA. (c) $U = -1.03$ V, and $I = 32.2$ pA.

activation strategy, we found that the dissymmetric dehalogenation reaction can also be steered by pre-self-assembly.

4,4'-Dibromo-*p*-terphenyl (denoted as DBTP) has attracted a great deal of attention because of its ability to fabricate atomically precise graphene nanoribbons on noble metal surfaces.^{32,35} In this work, we report the detailed formation of organometallic dimers of the dissymmetric dehalogenation reaction on Ag(111) that originated from a symmetric precursor and reveal that the self-assembly structures can rationally control the reaction pathways. The DBTP molecule was chosen as the precursor for the dissymmetric dehalogenation reaction (as shown in Scheme 1), which contains two Br atoms of the same chemical environment. Upon deposition of DBTP on a cold Ag(111) surface, the molecules can align and form two main phases of ordered structures. After self-assembled structure 1 (rectangular network) is annealed at room temperature (RT), only one C–Br bond of the DBTP molecule is cleaved, and we observe the formation of organometallic dimers formed by dissymmetric debromination, each dimer containing a C–Ag–C bond. Further annealing at a higher temperature leads to the formation of symmetric one-dimensional organometallic supramolecular wires and eventually covalent nanowires; this route is denoted as “pathway I” in Scheme 1. However, if the molecules preassembled into a self-assembled structure 2 (ladder phase), the DBTP molecules are more likely to convert into symmetric organometallic oligomers upon annealing at RT; this route is denoted as “pathway II” in Scheme 1. These reaction processes are

carefully monitored by STM, demonstrating that the pre-self-assembly structures play important roles in steering reaction pathways. More importantly, it provides a viable route toward dissymmetric activation of a mirror-symmetric molecule.

According to a previous study of DBTP on a Ag(111) surface, C–Br bond dissociation occurs at room temperature (and well below), resulting in the formation of organometallic chains.³⁴ To obtain unreacted DBTP monomers, DBTP molecules were deposited on a cold Ag(111) surface for 5 min after the Ag(111) sample was taken from the scanner (80 K) in the STM chamber to the sample holder in the preparation chamber (RT), and then the sample was transferred back to the STM chamber for scanning. In this way, physically adsorbed DBTP monomers can be obtained, and they self-assemble into a rectangular network (Figure 1a). Each rod in the STM image corresponds to a single DBTP molecule, with a measured length of 1.53 ± 0.05 nm, which is in accordance with the value from a previous report (1.52 nm).³⁴ In addition, the shape of the rod matches well with that of the DBTP molecule observed in the previous report.³⁵ Two obvious protrusions at terminals of rod are ascribed to Br atoms, indicating that the C–Br bond is present. We first discuss the molecular alignments in the rectangular self-assembled phase. This self-assembled structure formed by DBTP molecules has been reported by Chung et al.³⁶ and interpreted as a result of the self-assembly of intact DBTP molecules mainly governed by Br...Br and Br...H bonds, which are indicated in the corresponding schematic structural models

(Figure 1a) by black and green dashed lines, respectively. The square unit cell is outlined in Figure 1a with the following measured parameters: $a = b = 2.75 \pm 0.05$ nm, and $\alpha = \beta = 90^\circ$. One thing we need to note is that in the rectangular phase, two chiral nodes are observed, which are formed by four DBTP molecules aggregated in a head-to-head manner into rotary clockwise and anticlockwise quartet structures. These nodes have been observed in a previous study,³⁶ in which the internal structures of nodes could hardly be clearly observed. In this work, four brighter protrusions within these nodes can also be distinguished, indicating the presence of C–Br bonds. To induce the transformation of rectangular phase, the cold sample was transferred to the sample holder (RT) again for 2 h without external heating and then transferred back to the STM scanner. We observed the formation of a new ordered rhombic network structure on the surface. A representative STM image is displayed in Figure 1b. To confirm the composition of this ordered structure, a high-resolution STM image of the edge of the ordered island was acquired as shown in Figure 1c. We found that there are many discrete rods near the rhombic network, which are highlighted by white contours. The rhombic network consists of uniform rods, and the rod structure is composed of two lobes (each attributed to a DBTP molecule with one end debrominated) and a single protrusion in the middle (attributed to the silver adatom). Silver and bromine atoms are denoted by green and white arrows, respectively. As it has been reported that the aryl bromides usually form the C–Ag–C species after debromination on a Ag(111) surface at RT,³⁴ the rod structure is naturally assigned to the organometallic intermediate, which is the product of dissymmetric debromination of two DBTP molecules. This organometallic intermediate is denoted as a dimer. Moreover, we also performed a density functional theory (DFT) calculation to optimize this expected intermediate structure in the gas phase (shown in the inset of Figure 1c), and the calculated length of the dimer is 3.08 nm, which agrees well with those observed in the STM image of 3.10 nm. These organometallic dimers assemble into a rhombic network with the following lattice parameters: $a = b = 2.71 \pm 0.05$ nm, and $\alpha = 84^\circ$. The unit cell of this structure is marked in Figure 1b. The corresponding schematic structural model is superimposed on the STM image. The formed rhombic networks are most likely stabilized by C–Br...H hydrogen bonds and C–Br...Ag interaction. Because the bromine end of the organometallic dimer points to the central silver of another dimer, the C–Br...Ag interaction should play a key role in the stabilization of this network. A similar case has been reported previously.³⁷

To exploit the relationship between the reaction product and pre-self-assembly, we compare the structures before and after the dissymmetric dehalogenation. Figure 1a shows the rectangular network, which has a square unit cell with parameters of 2.75 nm, consisting of four DBTP molecules. The unit cell parameters of the rhombic network [2.71 nm (Figure 1b)] are comparable to those of the rectangular self-assembly, and the molecular densities of these two phases also are almost identical, which means a potential relationship between them. For the sake of clarity, the DBTP molecules of two different orientations are colored red and green. The green (red) contours in panels a and b of Figure 1 explain the relation between the pre-self-assembly structure and the rhombic network, in which case one green (red) monomer reacts with another green (red) monomer at the opposite

position in the same node and therefore induces the formation of rhombic network. According to all of the observed phenomena described above, it is inevitable that the assembly structure of the dimer rhombic network is transformed from pre-self-assembly.

To study the Ullmann coupling step by step, we annealed the sample at an increased temperature (403 K) to induce complete debromination and the subsequent formation of symmetric one-dimensional organometallic chains (see Figure 2a) based on C–Ag–C bonds. It is noteworthy that the chains

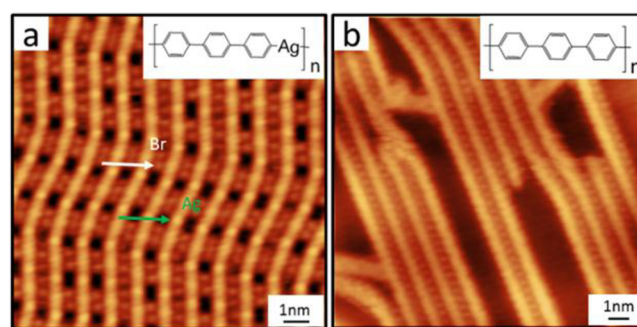


Figure 2. STM images of the Ag(111) surface after annealing. (a) STM image showing the formation of the C–Ag–C symmetric organometallic wires after the sample was annealed to 403 K, which are stabilized laterally by bromine atoms. Br and Ag atoms are denoted by white and green arrows, respectively. (b) The final annealing at 503 K gives rise to covalent supramolecular nanowires. The schematic models are indicated on the corresponding STM images. (a) $U = -1.03$ V, and $I = 26.3$ pA. (b) $U = -1.03$ V, and $I = 13.8$ pA.

are not straight and flat, different from those reported previously on a Ag(111) surface.³⁴ Further annealing at 503 K leads to the ejection of silver atoms from the organometallic bond. Figure 2b shows an STM image of the final product, in which molecular units are linked laterally by C–C covalent bonds and form supramolecular organic nanowires. According to previous studies on a metal surface, the parallel nanowires are stabilized by interchain C–H...Br...H–C interactions (Br atoms can be resolved near nanowires) and the detached Br atoms again act as “glue” to help the reaction products in an ordered way.³⁸

To further investigate the effect of pre-self-assembly, DBTP molecules were deposited on the same cold Ag(111) surface for 5 min [the Ag(111) sample was taken from the scanner (80 K) to the sample holder (RT)], which is different from the former case, and the sample continued to be placed on the sample holder for an additional 1 h without external heating. Interestingly, a new ordered network structure can be found on the surface. Figure 3a is a high-resolution image showing details of the ladder network, where Br atoms can be clearly resolved as bright spots at the end of each molecule, consistent with the same molecule as observed on Au(111), which reveals that the rod is still an unreacted monomer.³³ We note that in a previous study of DBTP on a Ag(111) surface, C–Br bond dissociation occurs at RT,³⁴ which is different from our case in which the sample temperature gradually increases from 80 K and may not reach RT after the cold Ag(111) is placed on the sample holder for a total of 65 min, so the unreacted monomers can be obtained. This closely packed self-assembled structure has not been observed on a Ag(111) surface in previous reports. Each unit cell consists of two DBTP

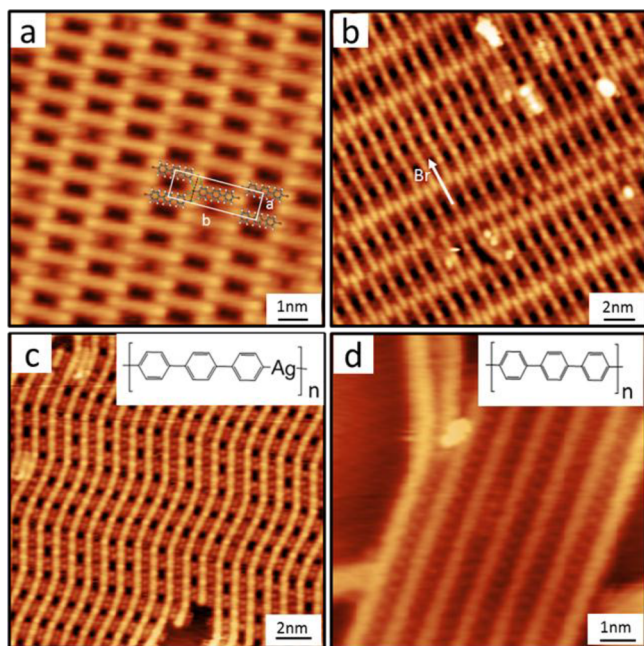


Figure 3. Reaction process of pathway II on Ag(111). (a) Self-assembled structure 2 (ladder network) of the intact species. (b) Annealing of a sample with a ladder network loaded at RT for 2 h. (c) Annealing at 403 K leads to full debromination and formation of organometallic wires. (d) Final annealing to 503 K gives rise to covalent nanowires. (a) $U = -1.10$ V, and $I = 13.5$ pA. (b) $U = -1.21$ V, and $I = 20.9$ pA. (c) $U = -1.03$ V, and $I = 13.8$ pA. (d) $U = -1.03$ V, and $I = 26.7$ pA.

molecules in parallel; the rectangular unit cell is outlined in Figure 3a with the following measured parameters: $a = 0.92 \pm 0.05$ nm, $b = 2.88 \pm 0.05$ nm, and $\alpha = \beta = 90^\circ$. This pattern is most likely stabilized by four lateral Br \cdots H bonds and two Br \cdots Br bonds, as represented by green and black dashed lines in the schematic structural model of Figure 3a, respectively. A similar structure has been observed on the Au(111) surface.³³ To study the reaction of a new structure, the sample with only a ladder network was placed on the sample holder for 2 h without external heating as in the rectangular phase, and the ladder network was partly transformed into ladder organometallic oligomers without any rhombic network appearing. Typical STM images of the organometallic oligomers are shown in Figure 3b. The supermolecules have prominent protrusions in the STM image, which is consistent with the characteristics of the organometallic intermediates connected by C–Ag–C bonds at the expense of the C–Br ones. This ladder assembled phase is more likely to induce the symmetric dehalogenation reaction, and dimers or oligomers with long-range ordering can be identified on surface, which are parallel to each other (see Figure 3b). Meanwhile, dot pairs located between the organometallic oligomers are Br atoms detached from DBTP. The dissociated bromine atoms are indicated by the arrow in Figure 3b. These detached Br atoms tend to form weak hydrogen bonds with adjacent H atoms in nearby benzene rings, which act as “glue” to help the supramolecular chains in parallel.³⁸ To complete the Ullmann coupling, we annealed the sample at 403 and 503 K. One-dimensional organometallic chains and continuous linear chains are observed on the surface, and the corresponding STM images are shown in panels c and d of Figure 3, respectively.

Previous works about DBTP molecules usually reported the observation of long organometallic chains after debromination on a silver surface at RT,³⁴ and our direct observation of dissymmetric debromination on a surface is the first report of its kind. In view of that, we speculate about the potential mechanism of intermediate formation. Although two bromine atoms are equivalent in molecular structure, C–Br bond cleavage always occurs in step-by-step manner.³⁹ However, the molecules are usually observed to be fully debrominated on reactive Ag(111), and the dissymmetric debromination on Ag(111) can be triggered only through appropriate thermal activation. As previously reported, when a C–X bond at one side is cleaved, a C–Ag bond forms immediately, and this product is short-lived and hard to resolve experimentally.⁴⁰ As soon as two molecules meet, one dimer that contains a C–Ag–C organometallic bond forms and the other C–Br bond of each DBTP molecule remains, which therefore results in the dissymmetric debromination. When dimer intermediates self-assemble, their diffusion and rotation are restricted by the self-assembly, and full dehalogenation will also be prevented by self-assembly.⁴¹ Thus, if the temperature is not high enough to overcome this diffusion barrier, only one C–Br bond can be cleaved and the dimer intermediate stably exists. Moreover, a comparison between the adsorption of DBTP on Ag(111) at low temperature and RT renders a significant difference. The DBTP molecules diffuse freely at the surface until reaction, and the C–Br bond is cleaved directly before self-assembly due to the higher reaction temperature, and subsequently construct 1D organometallic chains at RT, while no dimer rhombic network was observed.³⁴

Comparing the experimental results of the two cases presented above, we find that the reaction pathways for the Ullmann coupling can be controlled by pre-self-assembly. When DBTP molecules assemble into a rectangular network, each of the two nearby molecules in line is separated by perpendicular molecules, so only intermediates no longer than two units can form in the rhombic network after annealing. In the ladder network, DBTP molecules arrange in a head-to-tail manner, so it is easier to form symmetric intermediates after annealing. These different results are induced by different levels of steric hindrance of molecular self-assembly. Therefore, it is rational to conclude that dehalogenation reactions can be steered by self-assembly structures of DBTP molecules.

In conclusion, we have studied the Ullmann reaction of DBTP molecules on Ag(111) using high-resolution STM in UHV. In our case, the self-assembled structures efficiently influence on-surface reaction pathways and the dissymmetric dehalogenation reaction is realized. The self-assembly of the reactants in a rectangular network undergoes a dissymmetric debromination prior to the formation of longer symmetric organometallic intermediates on the Ag(111) surface, while the ladder assembled phase is more likely to induce the symmetric debromination reaction and convert into the symmetric organometallic intermediate. This is an important finding for providing valuable guidelines for the design of halogenated monomers suitable for realizing dissymmetric chemical reactions and paving new avenues for advancing the emerging field of on-surface synthesis.

METHODS

STM measurements were performed with a Unisoku low-temperature scanning tunneling microscope (LT SPM1200) operated in an ultra-high-vacuum (UHV) chamber (basic

pressure of 1×10^{-10} Torr) at 80 K. The Ag(111) substrate was prepared by several cycles of 1.0 keV Ar⁺ sputtering followed by annealing to 773 K until the surface was clean. Commercially available DBTP was loaded in a tantalum crucible, which was mounted in a molecular evaporator, and was thoroughly degassed for several hours before being deposited onto the substrate. A cold Ag(111) sample was taken from the scanner in the STM chamber (80 K) to the sample holder in the preparation chamber (RT), onto which molecules were deposited for 5 min. All STM measurements were carried out at 80 K, and all STM images were recorded in constant current mode using a tungsten tip. The sample temperature was measured using an infrared thermometer.

DFT calculations were carried out using Vienna Ab Initio Simulation Package (VASP) code within the Projector augmented-wave (PAW) scheme.⁴² The Perdew–Burke–Ernzerhof (PBE) functional was used to describe the exchange–correlation energy between electrons.⁴³ The structure geometry was optimized until all forces were ≤ 0.03 eV/Å, and the convergence criterion of each electronic step was $\leq 1.0 \times 10^{-5}$ eV.

AUTHOR INFORMATION

Corresponding Authors

Zhibo Ma – State Key Laboratory of Molecular Reaction Dynamics, Dalian Institute of Chemical Physics, Chinese Academy of Science, Dalian 116023, Liaoning, P. R. China; Email: zhbma@dicp.ac.cn

Wei Xu – Interdisciplinary Materials Research Center and College of Materials Science and Engineering, Tongji University, Shanghai 201804, P. R. China; orcid.org/0000-0003-0216-794X; Email: xuwei@tongji.edu.cn

Xueming Yang – State Key Laboratory of Molecular Reaction Dynamics, Dalian Institute of Chemical Physics, Chinese Academy of Science, Dalian 116023, Liaoning, P. R. China; Department of Chemistry, Southern University of Science and Technology, Guangdong, Shenzhen 518055, P. R. China; orcid.org/0000-0001-6684-9187; Email: xmyang@dicp.ac.cn

Authors

Hui Lu – State Key Laboratory of Molecular Reaction Dynamics, Dalian Institute of Chemical Physics, Chinese Academy of Science, Dalian 116023, Liaoning, P. R. China; University of Chinese Academy of Sciences, Beijing 100049, P. R. China; orcid.org/0000-0003-4207-5599

Wenlong E – State Key Laboratory of Molecular Reaction Dynamics, Dalian Institute of Chemical Physics, Chinese Academy of Science, Dalian 116023, Liaoning, P. R. China; University of Chinese Academy of Sciences, Beijing 100049, P. R. China

Liangliang Cai – Interdisciplinary Materials Research Center and College of Materials Science and Engineering, Tongji University, Shanghai 201804, P. R. China

Complete contact information is available at:
<https://pubs.acs.org/10.1021/acs.jpcllett.9b03688>

Author Contributions

[†]H.L. and W.E. contributed equally to this work.

Notes

The authors declare no competing financial interest.

ACKNOWLEDGMENTS

The authors acknowledge financial support from the National Natural Science Foundation of China (Grants 21688102 and 21673236), the Strategic Priority Research Program of Chinese Academy of Science (Grant XDB17000000), and the National Key Research and Development Program of the MOST of China (Grant 2016YFA0200603).

REFERENCES

- (1) Zhong, D.; Franke, J. H.; Podiyanachari, S. K.; Blömker, T.; Zhang, H.; Kehr, G.; Erker, G.; Fuchs, H.; Chi, L. Linear Alkane Polymerization on a Gold Surface. *Science* **2011**, *334*, 213–216.
- (2) Cai, L.; Yu, X.; Liu, M.; Sun, Q.; Bao, M.; Zha, Z.; Pan, J.; Ma, H.; Ju, H.; Hu, S.; et al. Direct Formation of C–C Double-Bonded Structural Motifs by On-Surface Dehalogenative Homocoupling of gem-Dibromomethyl Molecules. *ACS Nano* **2018**, *12*, 7959–7966.
- (3) Lafferentz, L.; Eberhardt, V.; Dri, C.; Africh, C.; Comelli, G.; Esch, F.; Hecht, S.; Grill, L. Controlling on-surface polymerization by hierarchical and substrate-directed growth. *Nat. Chem.* **2012**, *4*, 215–220.
- (4) Zhang, H.; Lin, H.; Sun, K.; Chen, L.; Zagranyski, Y.; Aghdassi, N.; Duhm, S.; Li, Q.; Zhong, D.; Li, Y.; et al. On-Surface Synthesis of Rylene-Type Graphene Nanoribbons. *J. Am. Chem. Soc.* **2015**, *137*, 4022–4025.
- (5) Grill, L.; Dyer, M.; Lafferentz, L.; Persson, M.; Peters, M. V.; Hecht, A. S. Nano-architectures by covalent assembly of molecular building blocks. *Nat. Nanotechnol.* **2007**, *2*, 687–691.
- (6) Wang, T.; Lv, H.; Huang, J.; Shan, H.; Feng, L.; Mao, Y.; Wang, J.; Zhang, W.; Han, D.; Xu, Q.; et al. Reaction selectivity of homochiral versus heterochiral intermolecular reactions of prochiral terminal alkynes on surfaces. *Nat. Commun.* **2019**, *10*, 4122.
- (7) Wang, S.; Sun, Q.; Gröning, O.; Widmer, R.; Pignedoli, C. A.; Cai, L.; Yu, X.; Yuan, B.; Li, C.; Ju, H.; et al. On-surface synthesis and characterization of individual polyacetylene chains. *Nat. Chem.* **2019**, *11*, 924–930.
- (8) Lischka, M.; Michelitsch, G. S.; Martsinovich, N.; Eichhorn, J.; Rastgoo-Lahrood, A.; Strunskus, T.; Breuer, R.; Reuter, K.; Schmittel, M.; Lackinger, M. Remote functionalization in surface-assisted dehalogenation by conformational mechanics: organometallic self-assembly of 3,3',5,5'-tetrabromo-2,2',4,4',6,6'-hexafluorobiphenyl on Ag(111). *Nanoscale* **2018**, *10*, 12035–12044.
- (9) Liu, J.; Chen, Q.; Xiao, L.; Shang, J.; Zhou, X.; Zhang, Y.; Wang, Y.; Shao, X.; Li, J.; Chen, W.; et al. Lattice-Directed Formation of Covalent and Organometallic Molecular Wires by Terminal Alkynes on Ag Surfaces. *ACS Nano* **2015**, *9*, 6305–6314.
- (10) Zhang, Y. Q.; Kepčija, N.; Kleinschrodt, M.; Diller, K.; Fischer, S.; Papageorgiou, A. C.; Allegretti, F.; Björk, J.; Klyatskaya, S.; Klappenberger, F.; et al. Homo-coupling of terminal alkynes on a noble metal surface. *Nat. Commun.* **2012**, *3*, 1286.
- (11) Gao, H. Y.; Wagner, H.; Zhong, D.; Franke, J. H.; Studer, A.; Fuchs, H. Glaser Coupling at Metal Surfaces. *Angew. Chem., Int. Ed.* **2013**, *52*, 4024–4028.
- (12) Otero, G.; Biddau, G.; Sánchez-Sánchez, C.; Caillard, R.; López, M. F.; Rogero, C.; Palomares, F. J.; Cabello, N.; Basanta, M. A.; Ortega, J.; et al. Fullerenes from aromatic precursors by surface-catalysed cyclodehydrogenation. *Nature* **2008**, *454*, 865–868.
- (13) Treier, M.; Pignedoli, C. A.; Laino, T.; Rieger, R.; Müllen, K.; Passerone, D.; Fasel, R. Surface-assisted cyclodehydrogenation provides a synthetic route towards easily processable and chemically tailored nanographenes. *Nat. Chem.* **2011**, *3*, 61–67.
- (14) Wiengarten, A.; Seufert, K.; Auwärter, W.; Eciija, D.; Diller, K.; Allegretti, F.; Bischoff, F.; Fischer, S.; Duncan, D. A.; Papageorgiou, A. C.; et al. Surface-assisted Dehydrogenative Homocoupling of Porphine Molecules. *J. Am. Chem. Soc.* **2014**, *136*, 9346–9354.
- (15) Li, Q.; Yang, B.; Lin, H.; Aghdassi, N.; Miao, K.; Zhang, J.; Zhang, H.; Li, Y.; Duhm, S.; Fan, J.; et al. Surface-Controlled Mono/Diselective ortho C–H Bond Activation. *J. Am. Chem. Soc.* **2016**, *138*, 2809–2814.

- (16) Sun, Q.; Zhang, C.; Kong, H.; Tan, Q.; Xu, W. On-surface aryl–aryl coupling via selective C–H activation. *Chem. Commun.* **2014**, *50*, 11825–11828.
- (17) Cai, J.; Ruffieux, P.; Jaafar, R.; Bieri, M.; Braun, T.; Blankenburg, S.; Muoth, M.; Seitsonen, A. P.; Saleh, M.; Feng, X.; et al. Atomically precise bottom-up fabrication of graphene nanoribbons. *Nature* **2010**, *466*, 470–473.
- (18) Lu, H.; Wang, H.; E, W.; Dai, D.; Fan, H.; Ma, Z.; Yang, X. On-Surface Fabrication of Small-Sized Nanoporous Graphene. *J. Phys. Chem. C* **2019**, *123*, 14404–14407.
- (19) Sakaguchi, H.; Song, S.; Kojima, T.; Nakae, T. Homochiral polymerization-driven selective growth of graphene nanoribbons. *Nat. Chem.* **2017**, *9*, 57–63.
- (20) Bieri, M.; Nguyen, M. T.; Gröning, O.; Cai, J.; Treier, M.; Ait-Mansour, K.; Ruffieux, P.; Pignedoli, C. A.; Passerone, D.; Kastler, M.; et al. Two-Dimensional Polymer Formation on Surfaces: Insight into the Roles of Precursor Mobility and Reactivity. *J. Am. Chem. Soc.* **2010**, *132*, 16669–16676.
- (21) Fan, Q.; Wang, C.; Han, Y.; Zhu, J.; Kuttner, J.; Hilt, G.; Gottfried, J. M. Surface-Assisted Formation, Assembly, and Dynamics of Planar Organometallic Macrocycles and Zigzag Shaped Polymer Chains with C–Cu–C Bonds. *ACS Nano* **2014**, *8*, 709–718.
- (22) Wang, W.; Shi, X.; Wang, S.; Van Hove, M. A.; Lin, N. Single-Molecule Resolution of an Organometallic Intermediate in a Surface-Supported Ullmann Coupling Reaction. *J. Am. Chem. Soc.* **2011**, *133*, 13264–13267.
- (23) Walch, H.; Gutzler, R.; Sirtl, T.; Eder, G.; Lackinger, M. Material- and Orientation-Dependent Reactivity for Heterogeneously Catalyzed Carbon-Bromine Bond Homolysis. *J. Phys. Chem. C* **2010**, *114*, 12604–12609.
- (24) Krug, C. K.; Fan, Q.; Fillsack, F.; Glowatzki, J.; Trebel, N.; Heuplick, L. J.; Koehler, T.; Gottfried, J. M. Organometallic ring vs. chain formation beyond kinetic control: steering their equilibrium in two-dimensional confinement. *Chem. Commun.* **2018**, *54*, 9741–9744.
- (25) Dai, J.; Fan, Q.; Wang, T.; Kuttner, J.; Hilt, G.; Gottfried, J. M.; Zhu, J. The role of the substrate structure in the on-surface synthesis of organometallic and covalent oligophenylene chains. *Phys. Chem. Chem. Phys.* **2016**, *18*, 20627–20634.
- (26) Judd, C. J.; Haddow, S. L.; Champness, N. R.; Saywell, A. Ullmann Coupling Reactions on Ag(111) and Ag(110); Substrate Influence on the Formation of Covalently Coupled Products and Intermediate Metal–Organic Structures. *Sci. Rep.* **2017**, *7*, 14541.
- (27) Simonov, K. A.; Vinogradov, N. A.; Vinogradov, A. S.; Generalov, A. V.; Zagrebina, E. M.; Svirskiy, G. I.; Cafolla, A. A.; Carpy, T.; Cuniffe, J. P.; Taketsugu, T.; et al. From Graphene Nanoribbons on Cu(111) to Nanographene on Cu(110): Critical Role of Substrate Structure in the Bottom-Up Fabrication Strategy. *ACS Nano* **2015**, *9*, 8997–9011.
- (28) Peyrot, D.; Silly, F. On-Surface Synthesis of Two-Dimensional Covalent Organic Structures versus Halogen-Bonded Self-Assembly: Competing Formation of Organic Nanoarchitectures. *ACS Nano* **2016**, *10*, 5490–5498.
- (29) Zhou, X.; Dai, J.; Wu, K. Steering on-surface reactions with self-assembly strategy. *Phys. Chem. Chem. Phys.* **2017**, *19*, 31531–31539.
- (30) Huang, H.; Wei, D.; Sun, J.; Wong, S. L.; Feng, Y. P.; Neto, A. H. C.; Wee, A. T. S. Spatially Resolved Electronic Structures of Atomically Precise Armchair Graphene Nanoribbons. *Sci. Rep.* **2012**, *2*, 983.
- (31) Liu, J.; Chen, Q.; Cai, K.; Li, J.; Li, Y.; Yang, X.; Zhang, Y.; Wang, Y.; Tang, H.; Zhao, D.; Wu, K. Stepwise on-surface dissymmetric reaction to construct binodal organometallic network. *Nat. Commun.* **2019**, *10*, 2545.
- (32) Song, S.; Kojima, T.; Nakae, T.; Sakaguchi, H. Wide graphene nanoribbons produced by interchain fusion of poly(p-phenylene) via two-zone chemical vapor deposition. *Chem. Commun.* **2017**, *53*, 7034–7036.
- (33) Basagni, A.; Sedona, F.; Pignedoli, C. A.; Cattelan, M.; Nicolas, L.; Casarin, M.; Sambri, M. Molecules–Oligomers–Nanowires–Graphene Nanoribbons: A Bottom-Up Stepwise On-Surface Covalent Synthesis Preserving Long-Range Order. *J. Am. Chem. Soc.* **2015**, *137*, 1802–1808.
- (34) Chung, K. H.; Koo, B. G.; Kim, H.; Yoon, J. K.; Kim, J. H.; Kwon, Y. K.; Kahng, S. J. Electronic structures of one-dimensional metal–molecule hybrid chains studied using scanning tunneling microscopy and density functional theory. *Phys. Chem. Chem. Phys.* **2012**, *14*, 7304–7308.
- (35) Chung, K.-H.; Kim, H.; Jang, W. J.; Yoon, J. K.; Kahng, S. J.; Lee, J.; Han, S. Molecular Multistate Systems Formed in Two-Dimensional Porous Networks on Ag(111). *J. Phys. Chem. C* **2013**, *117*, 302–306.
- (36) Chung, K. H.; Park, J.; Kim, K. Y.; Yoon, J. K.; Kim, H.; Han, S.; Kahng, S. J. Polymorphic porous supramolecular networks mediated by halogen bonds on Ag(111). *Chem. Commun.* **2011**, *47*, 11492–11494.
- (37) Wang, T.; Lv, H.; Feng, L.; Tao, Z.; Huang, J.; Fan, Q.; Wu, X.; Zhu, J. Unravelling the Mechanism of Glaser Coupling Reaction on Ag(111) and Cu(111) Surfaces: a Case for Halogen Substituted Terminal Alkyne. *J. Phys. Chem. C* **2018**, *122*, 14537–14545.
- (38) Dai, J.; Zhao, W.; Xing, L.; Shang, J.; Ju, H.; Zhou, X.; Liu, J.; Chen, Q.; Wang, Y.; Zhu, J.; et al. Dechlorinated Ullmann Coupling Reaction of Aryl Chlorides on Ag(111): A Combined STM and XPS Study. *ChemPhysChem* **2019**, *20*, 2367–2375.
- (39) Fritton, M.; Duncan, D. A.; Deimel, P. S.; Rastgoo-Lahrood, A.; Allegretti, F.; Barth, J. V.; Heckl, W. M.; Björk, J.; Lackinger, M. The Role of Kinetics versus Thermodynamics in Surface-Assisted Ullmann Coupling on Gold and Silver Surfaces. *J. Am. Chem. Soc.* **2019**, *141*, 4824–4832.
- (40) Kawai, S.; Sadeghi, A.; Okamoto, T.; Mitsui, C.; Pawlak, R.; Meier, T.; Takeya, J.; Goedecker, S.; Meyer, E. Organometallic Bonding in an Ullmann-Type On-Surface Chemical Reaction Studied by High-Resolution Atomic Force Microscopy. *Small* **2016**, *12*, 5303–5311.
- (41) Zhou, X.; Wang, C.; Zhang, Y.; Cheng, F.; He, Y.; Shen, Q.; Shang, J.; Shao, X.; Ji, W.; Chen, W.; et al. Steering Surface Reaction Dynamics with a Self-Assembly Strategy: Ullmann Coupling on Metal Surfaces. *Angew. Chem., Int. Ed.* **2017**, *56*, 12852–12856.
- (42) Kresse, G.; Joubert, D. From ultrasoft pseudopotentials to the projector augmented-wave method. *Phys. Rev. B: Condens. Matter Mater. Phys.* **1999**, *59*, 1758–1775.
- (43) Perdew, J. P.; Burke, K.; Ernzerhof, M. Generalized Gradient Approximation Made Simple. *Phys. Rev. Lett.* **1996**, *77*, 3865–3868.